



Atractylodin alleviates nonalcoholic fatty liver disease by regulating Nrf2-mediated ferroptosis

Qingyan Ye^{a,1}, Yun Jiang^{b,1}, Di Wu^b, Jingwen Cai^c, Zhitian Jiang^d, Zhen Zhou^c, Liyan Liu^c, Qihua Ling^{c,*}, Qian Wang^{c,**}, Gang Zhao^{d,***}

^a Department of Paediatrics, Shuguang Hospital Affiliated to Shanghai University of Traditional Chinese Medicine, 528, Zhangheng Road, Shanghai 201203, China

^b Department of Hepatology, Shuguang Hospital Affiliated to Shanghai University of Traditional Chinese Medicine, 528, Zhangheng Road, Shanghai 201203, China

^c Department of Emergency Internal Medicine, Shuguang Hospital Affiliated to Shanghai University of Traditional Chinese Medicine, 528, Zhangheng Road, Shanghai 201203, China

^d Department of Outpatient and Emergency Office, Shuguang Hospital Affiliated to Shanghai University of Traditional Chinese Medicine, 528, Zhangheng Road, Shanghai 201203, China

ARTICLE INFO

Keywords:

NAFLD
Atractylodin
Ferroptosis
Nrf2

ABSTRACT

Nonalcoholic fatty liver disease (NAFLD) is the most common cause of chronic liver disease worldwide. Oxidative stress is one of the main inducers of NAFLD. Atractylodin (ART), a major active ingredient of *Atractylodes lancea*, possesses potential antioxidant and anti-inflammatory activity in many types of disease. In the current study, the underlying mechanism by which ART alleviates the progression of NAFLD was explored. The function of ART in facilitating NAFLD was investigated in vitro and in vivo. Functionally, ART attenuated high-fat diet (HFD)-induced NAFLD in mice and palmitic acid (PA)-induced oxidative stress in HepG2 cells. Furthermore, our data verified that ART attenuated HFD-induced NAFLD by inhibiting ferroptosis of hepatocyte cells, as evidenced by decreased Fe²⁺ concentration, reactive oxygen species (ROS) level, malondialdehyde (MDA) content, and increased glutathione (GSH) content. The protective effect of ART on the cell viability of hepatocytes was blocked by a specific ferroptosis inhibitor (ferrostatin-1). Mechanistically, ART treatment promoted the translocation of nuclear factor erythroid 2-related factor 2 (NFE2L2/NRF2) and thus increased glutathione peroxidase 4 (GPX4), ferritin heavy chain 1 (FTH1), and solute carrier family 7 member 11 (SLC7A11) expression. Taken together, ART alleviates NAFLD by regulating Nrf2-mediated ferroptosis.

1. Introduction

NAFLD is a prevalent chronic liver disease that often coexists with diabetes, hyperlipidaemia, and obesity. The prevalence of NAFLD worldwide is estimated to be 24%, of which 5–20% of patients with simple steatosis progress to nonalcoholic steatohepatitis

* Corresponding author.

** Corresponding author.

*** Corresponding author.

E-mail addresses: lingqihua@shutcm.edu.cn (Q. Ling), docqianwang@126.com (Q. Wang), drzhaogang@126.com (G. Zhao).

¹ These authors contributed equally to this work.

(NASH) [1–3]. Nonalcoholic steatohepatitis is characterized by hepatocellular lipid accumulation, lobular inflammation, and ballooning of hepatocytes in patients [4,5]. Although the underlying mechanisms that contribute to the development of NAFLD are still unclear, a multiple hit (inflammatory response, oxidative stress, and lipid accumulation) hypothesis has been proposed to elaborate the factors contributing to the pathological processes [6,7]. Therefore, exploring drugs with anti-inflammatory and antioxidative capacity will be beneficial for NAFLD therapy.

Numerous studies have shown that herbal extracts, such as resveratrol [8], salvianolic acid B [9], and curcumin [10], improve the occurrence and development of NAFLD through antioxidant effects. Atractylodin (ART), a bioactive monomer extract from *Atractylodes lancea* De Candolle, has many pharmacological properties, such as antioxidative [11] and anticancer properties [12]. ART has been reported to suppress the expression of mucin 5AC (MUC5AC) and extracellular matrix (ECM) in lipopolysaccharide (LPS)-induced airway inflammation by inhibiting the nuclear factor-kappaB (NF- κ B) pathway [13] and to inhibit the expression of interleukin 6 (IL-6) by blocking the activation of mitogen-activated protein kinases (MAPKs) in human mast cells (HMC-1 cells) [14]. In the current study, we found that ART treatment improves the pathological process of NAFLD by inhibiting oxidative stress. Thus, the mechanism underlying ART improving the pathological process of NAFLD has potential therapeutic implications.

Ferroptosis, a form of programmed cell death, is characterized by the accumulation of ions and ROS in the process of cell death [15]. Recently, a growing number of studies have suggested that ferroptosis can be induced by suppressing SLC7A11/xCT activity, downregulating GPX4, and accumulating ROS [16]. An increasing number of studies have demonstrated that ferroptosis contributes to the development of NAFLD. Qi Jing et al. found that ferroptosis was involved in the development of NAFLD by regulating lipid peroxidation-mediated cell death in mice [17]. Li Xiaoya et al. reported that ferroptosis inhibition alleviates MCD diet-induced NASH by suppressing liver lipotoxicity [18]. These studies suggest that new prevention and treatment strategies for NAFLD can be developed by regulating ferroptosis. In the current study, we explored the underlying mechanism by which ART alleviates the development of NAFLD by regulating ferroptosis.

2. Materials and methods

2.1. Animals and experiments

C57BL/6J male mice were purchased from SLAC Laboratory Animal Co., Ltd. (Shanghai, China). All animal experiments were approved by the Animal Ethics Committee of Shanghai Municipal Hospital of Traditional Chinese Medicine. Mice were housed in specific pathogen-free (SPF) conditions and were randomly divided into five groups ($n = 7$): control group (saline + 0.5% DMSO), HFD group (saline + 0.5% DMSO), ART-Low (ART-L 20 mg/kg, dissolved in 0.5% DMSO) group, ART-Medium (ART-M 40 mg/kg, dissolved in 0.5% DMSO) group, and ART-High (ART-H 80 mg/kg, dissolved in 0.5% DMSO) group. Mice were fed a normal chow diet (ND) consisting of 4.5% fat or a high-fat diet (HFD) consisting of 60% fat (D12492, Research Diets) for 16 weeks. After 8 weeks of HFD feeding, mice were intragastrically administered different doses of ART. The body weights of the mice were measured weekly. All animal experiments were approved by the Experimental Animal Ethics Committee of Shanghai University of Traditional Chinese Medicine, approval number PZSHUTCM191213004.

2.2. Measurement of serum TG, ALT, and AST

Serum triglycerides (TGs), alanine aminotransferase (ALT), and aspartate aminotransferase (AST) were assessed by an Elabscience assay kit (Elabscience, Wuhan, China) according to the manual.

2.3. Oil red O and haematoxylin and eosin (H&E) staining

For Oil Red O staining, the liver sections were washed with PBS and stained with Mayer's haematoxylin solution (Sigma, St. Louis, MO, USA). The liver sections were incubated with 60% isopropanol (Sigma) for 15 min and then stained with Oil Red O solution (Sigma).

For H&E staining, the liver samples were sliced into sections (8 μ m), fixed with 4% PFA at RT, and then stained with H&E staining solution for 10 min.

2.4. Oxidative stress index measurements

The ROS level was measured by 2,7-dichlorodihydrofluorescein diacetate (DCFH-DA) assay. In brief, liver tissue homogenate or cell lysate was incubated with 15 μ M DCFH-DA probe for 30 min in the dark at 37 $^{\circ}$ C, and then fluorescence was measured by a biosync bioreader 7000 (Germany). The content of malondialdehyde (MDA) in the liver tissue homogenate or cell lysate was measured according to the manufacturer's instructions. Superoxide dismutase (SOD) activity was determined by inhibiting the formation of formaldehyde from nitroblue tetrazole. The GSH content was measured by a GSH assay kit (Abcam) according to the manufacturer's instructions. The total protein concentration in liver tissue homogenate or cell lysate was measured using a BCA assay (Sigma).

2.5. Cell viability of HepG2 cells

HepG2 cells were maintained in DMEM supplemented with 2 mM glutamine, 10% foetal calf serum, and nonessential amino acids.

The cells were cultured at 37 °C under a 5% CO₂ atmosphere. HepG2 cells were treated with 0.25 mM palmitic acid (PA) for 24 h to establish NAFLD cell models. Cell viability was determined by Cell Counting Kit-8 (CCK-8) assay at different concentrations of ART (10, 20, 40 μM). Briefly, HepG2 cells were seeded into 96-well plates (5 *10³ cells/well), and 10 μL CCK-8 solution (Abcam) was added. Then, the cells were incubated at RT for 2 h. Absorbance was detected at a wavelength of 450 nm.

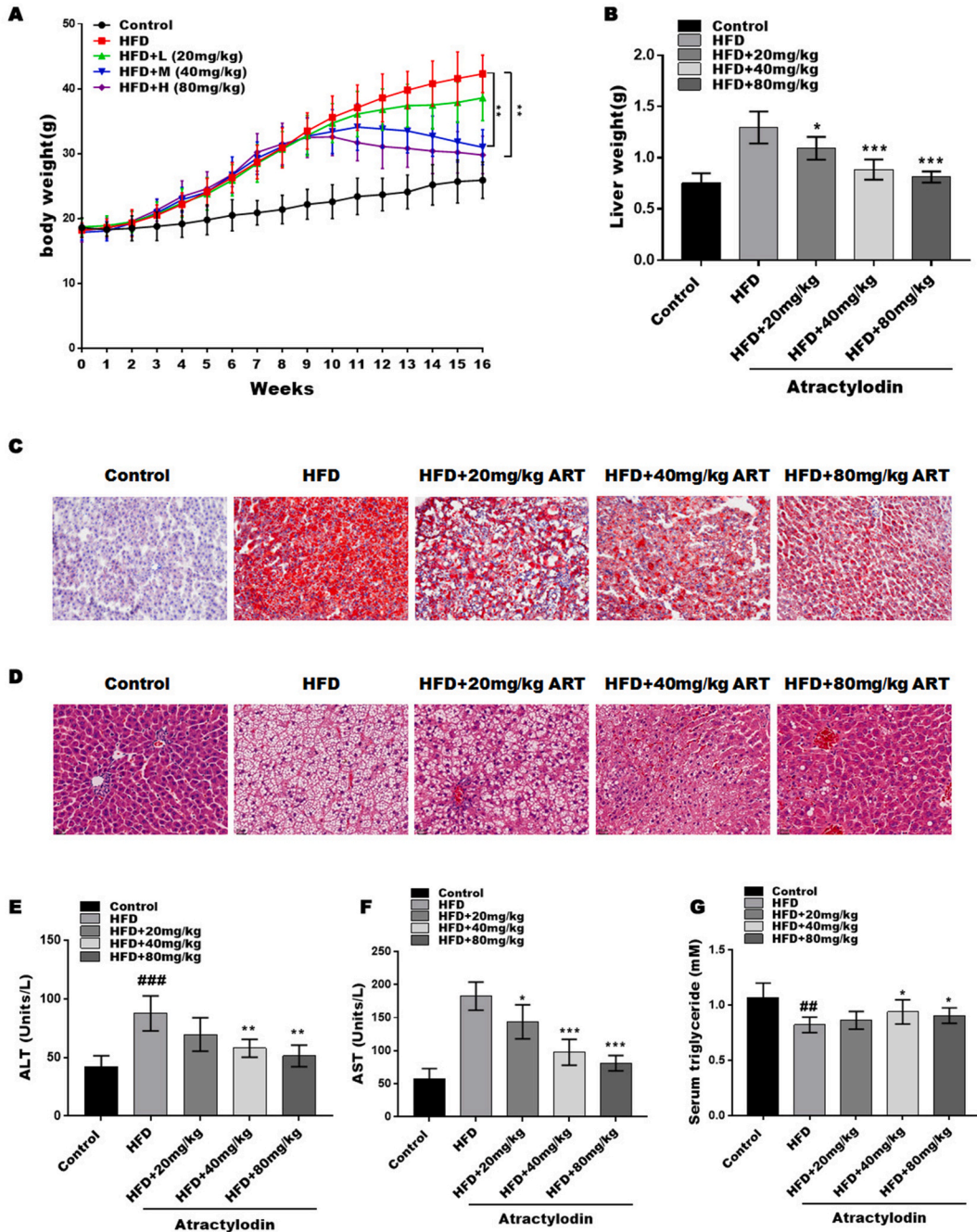


Fig. 1. Atractylodin attenuates HFD-induced NAFLD. HFD-induced NAFLD was established by 8 weeks of high-diet intervention and then treated with or without artactylodin for another 8 weeks. (A and B) Body weight (A) and liver weight (B) of mice. (C) The accumulation of lipids in the liver tissue of each group at 16 weeks was measured by oil red O staining. (D) Lipid accumulation in the liver tissue of each group at 16 weeks was evaluated by HE staining (n = 7). (E–G) Serum ALT, AST, and TG at 16 weeks were evaluated by ELISA. (n = 7); ##P < 0.01, ###P < 0.001, compared with the control group. *P < 0.05; **P < 0.01; ***P < 0.001, compared with the HFD group. (For interpretation of the references to colour in this figure legend, the reader is referred to the Web version of this article.)

2.6. Fluorescein diacetate (FDA) staining

HepG2 cells were cultured with 40 μ M FDA for 24 h, and then 10 μ l of FDA (5 mg/mL; Invitrogen, CA, USA) solution was added to the cells and incubated at 37 $^{\circ}$ C with 5% CO₂ for 20 min. Then, cell images were obtained using a fluorescence microscope (Olympus Corporation, Japan).

2.7. Western blotting

For ferroptosis analysis, HepG2 whole cells from each group (control, PA, and PA + ART) were lysed by using RIPA buffer (Beyotime, Shanghai, China). The concentration of protein was determined by a commercial BCA kit (Sigma). Approximately 20 μ g of protein was loaded on 8% polyacrylamide gradient gels (Beyotime) and transferred to PVDF membranes (Thermo Fisher). The transferred membranes were blocked with 1% nonfat milk solution at RT for 1 h and then incubated with anti-GPX4 (1:1000; ab125066, Abcam), anti-SLC7A11 (1:1000; ab238969, Abcam), anti-FTH1 (1:1000; ab183781, Abcam), and anti-actin (1:5000;

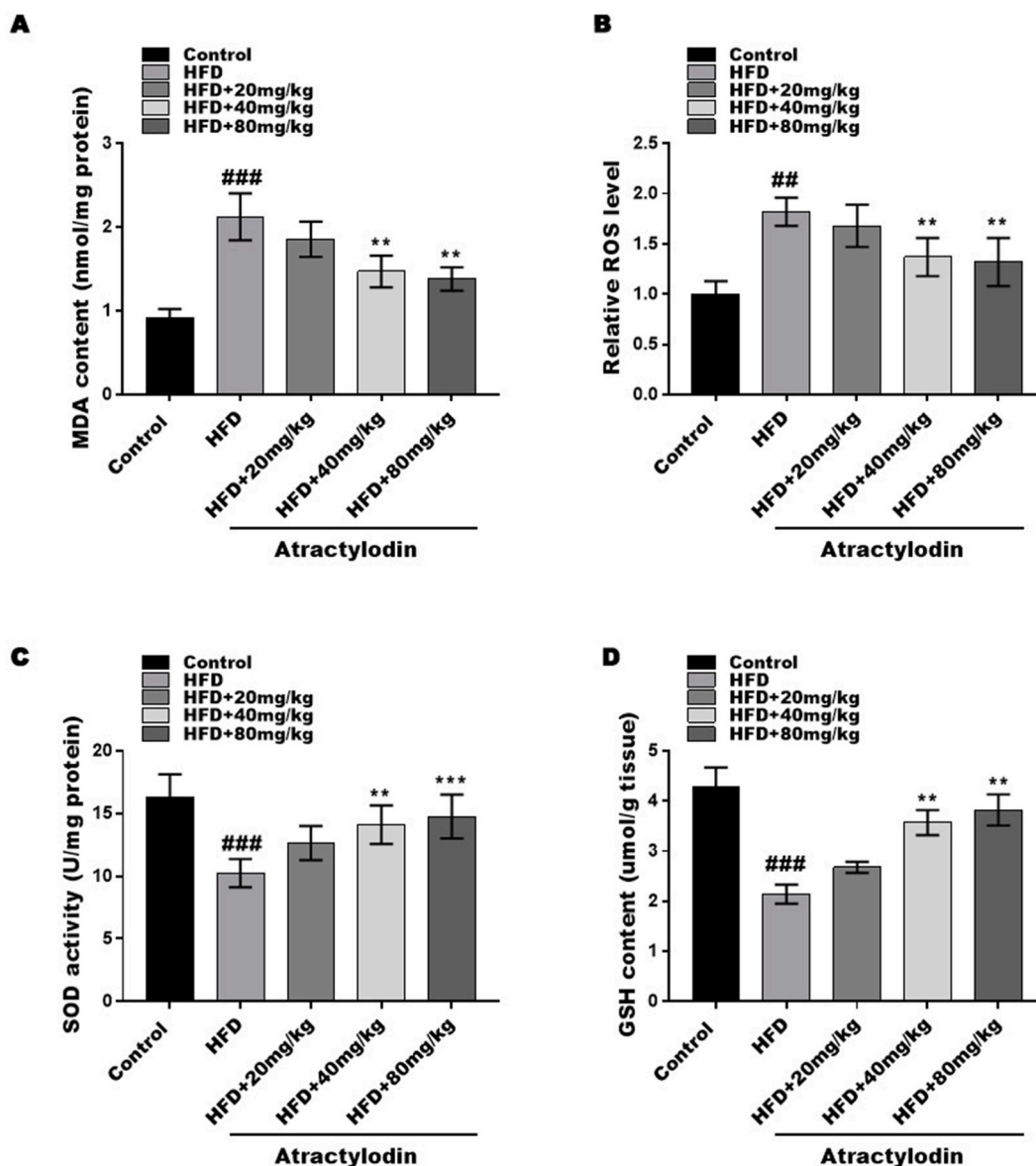


Fig. 2. Atractylodin attenuates HFD-induced oxidative stress. The content of MDA (A), the levels of ROS (B), the activity of SOD (C) and the content of GSH (D) were assessed by commercial kits. ###P < 0.001 and ##P < 0.01 compared with the control group. **P < 0.01, ***P < 0.001, compared with the HFD group.

ab5694, Abcam) at 4 °C overnight. The next day, the membranes were washed with TBST three times. Then, the membranes were labelled with HRP-conjugated goat anti-rabbit IgG antibody (1:3000; S0010; Affinity Biosciences) at RT for 90 min after washing with TBST three times. The immunoblots were visualized using an enhanced chemiluminescence solution.

For Nrf2 activation analysis, the nuclear and cytoplasmic proteins of HepG2 cells were isolated by nuclear and cytoplasmic protein extraction kits (Beyotime. Shanghai, China). Approximately 20 µg nuclear protein and cytoplasmic protein were loaded on 8% polyacrylamide gradient gels (Beyotime) and transferred to PVDF membranes (Thermo Fisher). The transferred membranes were blocked with 1% nonfat milk solution at RT for 1 h and then incubated with NRF2 (1:1000; ab137550, Abcam), anti-lamin B (1:500; ab32535, Abcam), and anti-actin (1:5000; ab5694, Abcam) at 4 °C overnight. Then, the membranes were labelled with HRP-conjugated goat anti-rabbit IgG antibody (1:3000; S0010; Affinity Biosciences) at RT for 90 min after washing with TBST three times. The immunoblots were visualized using an enhanced chemiluminescence solution.

2.8. Statistical analysis

SPSS 20.0 software (IBM, NY, USA) was used for statistical analyses in this study. All the data are expressed as the mean ± standard deviation (SD). The significance between two groups was determined by Student’s t-test, and more than two groups were determined by one-way ANOVA followed by Tukey–Kramer multiple comparisons test. $p < 0.05$ was considered to indicate a statistically significant difference.

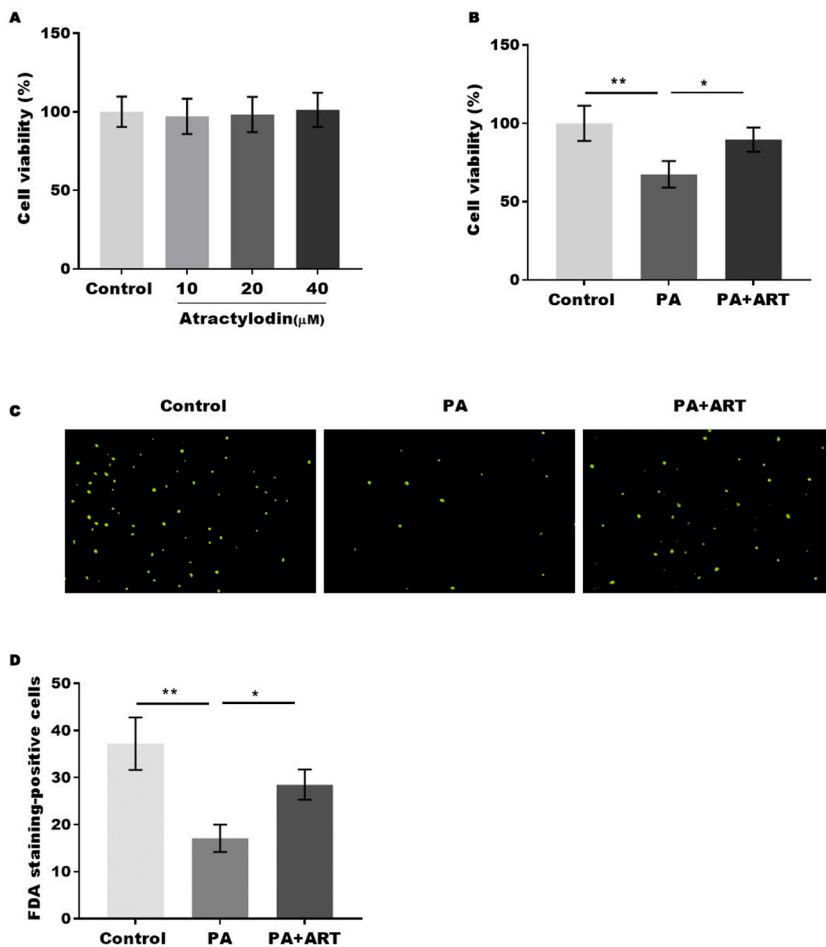


Fig. 3. Atractylodin promotes cell viability in the NAFLD in vitro model. (A) Cell cytotoxicity of ART on HepG2 cells was assessed by CCK-8 assay. (B) Cell viability of HepG2 cells treated with PA in the presence or absence of ART was assessed by CCK-8. (C) The cell death of HepG2 cells was assessed by FDA staining. $*p < 0.05$, $**p < 0.01$.

3. Result

3.1. Atractylodin attenuates HFD-induced NAFLD

We established an HFD-induced NAFLD mouse model. After 8 weeks of high-diet intervention, the HFD group showed a marked increase in body weight compared with the control group. Subsequently, the HFD mice were divided into four groups and given different interventions (low, 20 mg/kg ART (ART-L); medium, 40 mg/kg ART (ART-M); high, 80 mg/kg ART (ART-H) for 8 weeks. ART at different concentrations (20, 40, 80 mg/kg) markedly decreased body weight compared to the HFD group alone (Fig. 1A), and the 80 mg/kg ART treatment showed the greatest inhibition of body weight gain. The liver weight was markedly increased in the HFD mouse model compared with the control group, whereas this effect was partly blocked by ART treatment (Fig. 1 B).

Next, the fat accumulation and cell death of the liver in the different groups were assessed by Oil Red O and HE staining. HFD-fed

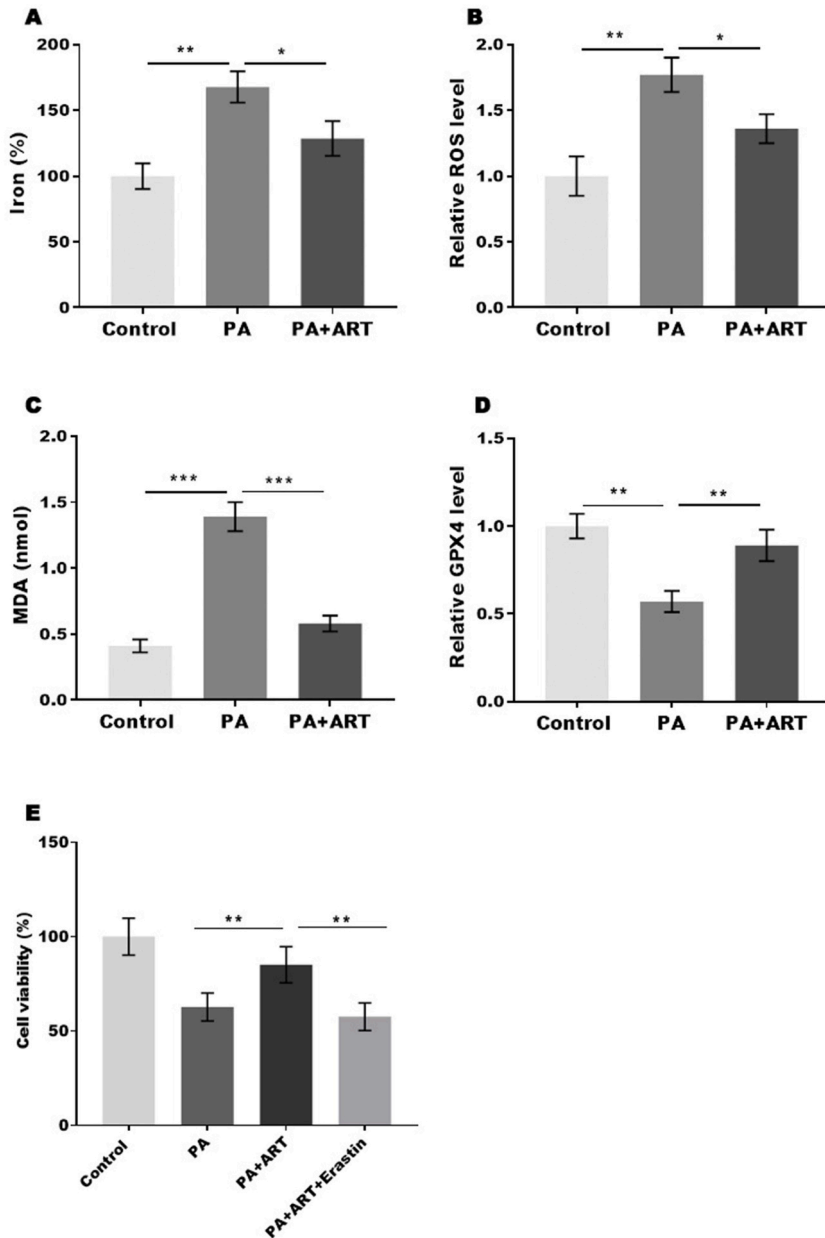


Fig. 4. Atractylodin promotes cell viability in the NAFLD cell model by inhibiting ferroptosis. (A-D) The percentage of iron (A), the levels of ROS (B), the content of MDA (C) and the content of GSH (D) were assessed by commercial kits. (E) The viability of HepG2 cells was assessed by CCK-8 assay. * $p < 0.05$, ** $p < 0.01$, *** $p < 0.001$.

mice exhibited marked increases in liver steatosis and lipid droplets, which were attenuated by ART treatment, indicating that ART treatment reduces excessive liver steatosis and lipid droplets in hepatocytes (Fig. 1C). Similarly, the HE data showed that liver steatosis and lipid droplets were significantly increased by HFD feeding; however, ART treatment decreased liver steatosis and lipid droplets. Next, the serum liver injury markers alanine aminotransferase (ALT), aspartate aminotransferase (AST), and triglyceride (TG) were assessed in the NAFLD mouse model. The release of ALT and AST into the serum reflects the degree of hepatocyte death. The levels of AST and ALT were markedly increased in the NAFLD model, while the level of TG was markedly decreased, reflecting the degree of hepatocyte death. ART treatment reversed these effects, suggesting that ART treatment attenuated hepatocyte injury and liver steatosis (Fig. 1E–G).

3.2. Atractyloidin attenuates HFD-induced oxidative stress

Oxidative stress and lipid peroxidation have been implicated in the development of NAFLD. To investigate the effects of ART on oxidative stress in the liver, we analysed ROS levels, MDA content, GSH content, and SOD activity. The HFD mice exhibited significantly higher ROS levels and MDA content compared to the control group, which were significantly reduced after ART treatment (Fig. 2A and B). Additionally, the GSH content and SOD activity were significantly decreased in the HFD mouse model but were markedly increased after ART treatment (Fig. 2C and D). These results suggest that ART treatment effectively attenuates oxidative stress induced by HFD in mice.

3.3. Atractyloidin promotes cell viability in the NAFLD in vitro model

To explore the effect of ART on cell death in NAFLD, PA-treated HepG2 cells were established as a NAFLD cell model. First, the cell cytotoxicity of ART on HepG2 cells was assessed by the CCK-8 assay. We found that 40 μ m ART displayed no cytotoxicity on HepG2 cells (Fig. 3A). Next, the cell viability of HepG2 cells treated with PA with or without ART treatment was assessed by CCK-8, and our data indicated that ART (40 μ m) treatment significantly reversed PA-induced cell viability inhibition in HepG2 cells, suggesting that ART has a protective effect against PA-induced cell death (Fig. 3B). The protective effect of ART on PA-induced cell death of HepG2 cells was further confirmed by FDA staining (Fig. 3C and D).

3.4. Atractyloidin promotes cell viability in the NAFLD cell model by inhibiting ferroptosis

Our results demonstrate that ART can inhibit oxidative stress and thereby attenuate cell ferroptosis in the liver tissue of mice. We further investigated the effects of ART on HepG2 cell ferroptosis. We analysed the markers of ferroptosis, including iron concentration, ROS level, MDA level, and GPX4 level. Our results showed that PA treatment significantly increased the concentration of iron, level of ROS, and content of MDA in HepG2 cells, while ART treatment restored these effects (Fig. 4A–C). Conversely, PA treatment decreased GPX4 expression, and this effect was reversed by ART treatment (Fig. 4D). To further confirm that ART regulates HepG2 cell viability by inhibiting ferroptosis, we treated a NAFLD cell model with ART in the presence or absence of erastin, an activator of ferroptosis. Our data revealed that the protective effect of ART was blocked by erastin, suggesting that ART promotes the viability of hepatocyte cells by inhibiting ferroptosis (Fig. 4E).

3.5. Atractyloidin suppresses the ferroptosis of hepatocytes induced by PA in vitro

To further verify that ART suppressed ferroptosis in PA-treated HepG2 cells, we analysed the expression of ferroptosis-associated

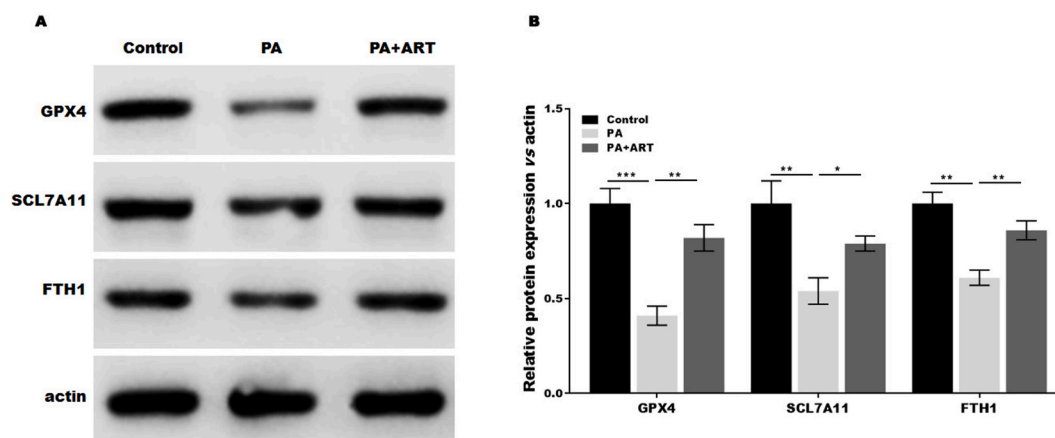


Fig. 5. Atractyloidin suppresses the ferroptosis of hepatocytes induced by PA in vitro. Western blotting analysis and semiquantitative analysis of GPX4, SCL7A11, and FTH1 protein levels in HepG2 cells treated with PA in the presence or absence of ART. * $p < 0.05$, ** $p < 0.01$, *** $p < 0.001$.

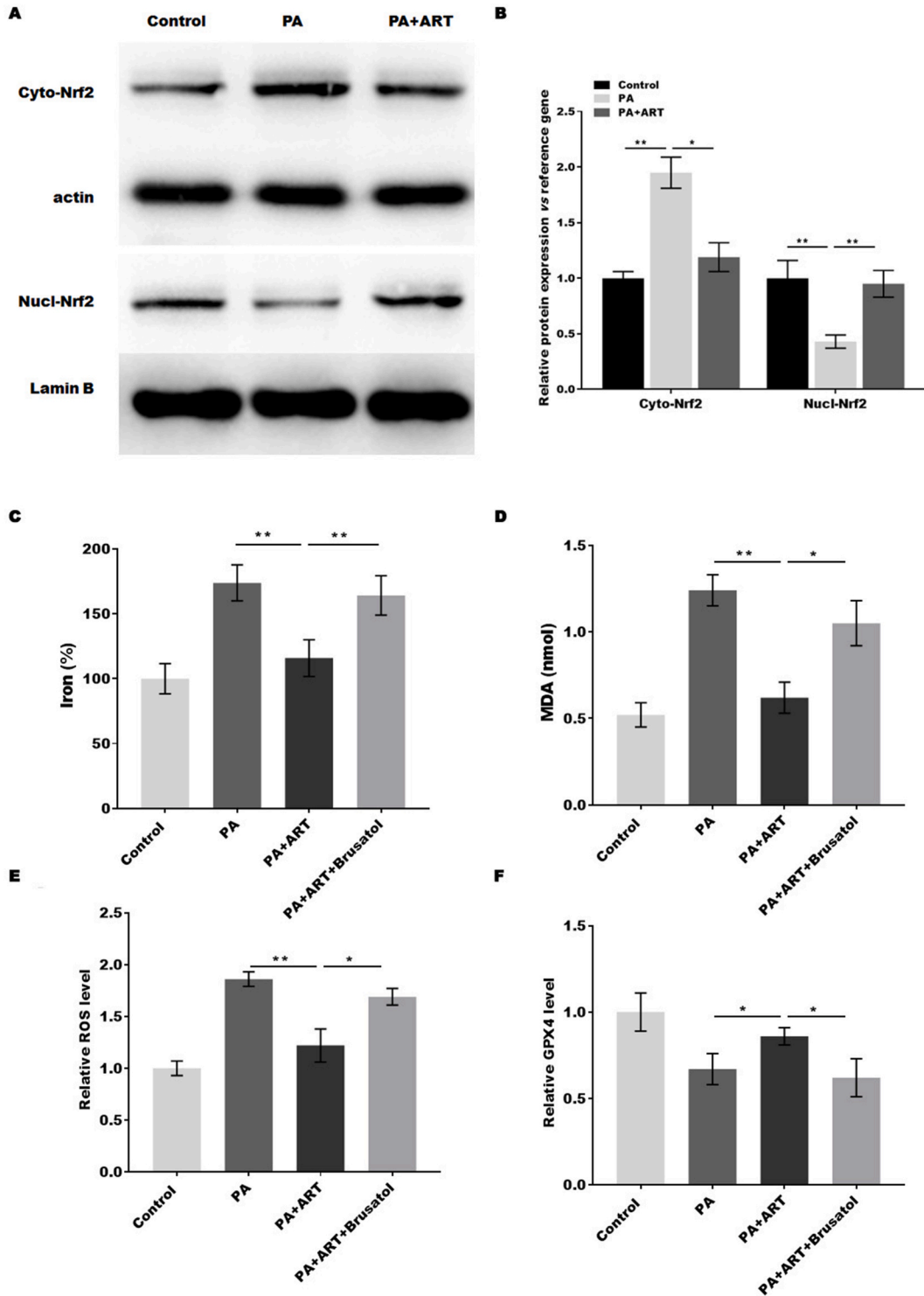


Fig. 6. Atractylodin suppresses hepatocyte ferroptosis by regulating Nrf2. (A and B) Western blotting analysis (A) and semiquantitative analysis (B) of cytoplasmic Nrf2 and nuclear Nrf2 protein levels in HepG2 cells treated with PA in the presence or absence of ART. (C–F) The percentage of iron (C), the content of MDA (D), the levels of ROS (E), and the content of GSH (F) were assessed by commercial kits. * $p < 0.05$, ** $p < 0.01$, *** $p < 0.001$.

proteins in the presence or absence of ART. Our results showed that PA treatment decreased the expression of GPX4, SLC7A11, and FTH1 compared to the control group, while the effect was restored by ART treatment (Fig. 5A and B). These findings support that ART inhibits ferroptosis in hepatocytes by increasing the expression of SLC7A11, GPX4, and FTH1.

3.6. Atractylodin suppressed the ferroptosis of hepatocytes by regulating Nrf2

A previous study showed that Nrf2-mediated signalling pathways were upregulated by atractylodin [11]. The expression of GPX4, SLC7A11, and FTH1 is regulated by Nrf2 [19], and Nrf2 is closely associated with NAFLD [20]. The activation of Nrf2 was analysed in PA-treated HepG2 cells with or without ART. The expression of Nrf2 was significantly increased by PA treatment, while the effect was blocked by ART (Fig. 6A and B). In addition, ART treatment markedly promoted Nrf2 translocation to the nucleus, indicating that ART suppressed the ferroptosis of hepatocytes in vitro by activating Nrf2. Next, we investigated whether Nrf2 mediates the function of ART by mediating hepatocyte ferroptosis. The dysregulation of ferroptosis markers (MDA, ROS, iron, and GPX4) induced by PA was blocked by ART, while the effect was restored by the Nrf2 inhibitor brusatol, indicating that ART suppressed the ferroptosis of hepatocytes by regulating Nrf2.

4. Discussion

NAFLD is a prevalent chronic liver disease closely related to obesity, inflammation, and oxidative stress [21]. Although the pathogenesis is complicated, it is clear that the cell death of hepatocytes plays an important role in the development of NAFLD [22]. Atractylodin has been previously shown to improve acute liver failure induced by D-galactosamine and LPS, possibly through its anti-inflammatory and antioxidative properties. However, the specific mechanism by which atractylodin improves NAFLD remains unclear. In this study, we aimed to investigate the effects of atractylodin on NAFLD and its underlying mechanism. Our findings suggest that atractylodin alleviates HFD-induced NAFLD by reducing oxidative stress and promoting cell viability. Moreover, atractylodin inhibited ferroptosis in vitro, leading to improved cell viability in a NAFLD cell model.

Numerous studies have established a correlation between oxidative stress induced by reactive oxygen species (ROS) and over 200 diseases, including nonalcoholic fatty liver disease (NAFLD). ROS-induced oxidative stress is known to contribute to the initiation and progression of NAFLD by disrupting cellular functions and ultimately leading to cell death [23]. Prior research has highlighted the role of oxidative stress in NAFLD and its mitigation through various mechanisms. For example, Li et al. clarified that haem oxygenase-1 alleviates NAFLD by inhibiting ROS-dependent endoplasmic reticulum stress [24]. Kim et al. demonstrated that GPx7 improves NAFLD by regulating oxidative stress [25]. Geng et al. found that metformin protects against PA-induced hepatic cell death by recovering mitochondrial function, decreasing cellular ROS production, and inducing SOD2 expression [26]. Recent studies have identified ART as a potential treatment for acute liver injury by inhibiting ROS production through upregulation of HO-1 and NQO1 expression [11]. In the current study, we demonstrate that ART suppresses liver steatosis and lipid droplets in NAFLD mice and reduces ROS production. Furthermore, we show that ART mitigates hepatic cell death induced by ROS production in vitro, suggesting its potential in mitigating oxidative stress in NAFLD.

Ferroptosis, a form of cell death, is known to occur alongside iron accumulation and ROS production during the cell death process. Research has identified ferroptosis as a significant contributor to the development of nonalcoholic steatohepatitis (NASH) and as the trigger for initiating inflammation in NASH. For example, Qi et al. reported that ferroptosis contributes to the development of nonalcoholic steatohepatitis (NASH) by regulating lipid peroxidation-mediated cell death in mice [17]. Tsurusaki et al. demonstrated that hepatic ferroptosis plays an important role as the trigger for initiating inflammation in NASH [27]. Our study shows that ART attenuates the development of NAFLD by inhibiting ferroptosis, as evidenced by the blockage of the protective function of ART on hepatocytes by a ferroptosis activator. Furthermore, ART treatment restored the expression of GPX4, SLC7A11, and FTH1, which are all associated with ferroptosis.

NRF2 is a key negative regulator of ferroptosis and is known to regulate the expression of GPX4, SLC7A11, and FTH1. Moreover, Nrf2 plays an important role in the development of NAFLD [20,28]. Therefore, we assumed that ART regulates ferroptosis through the Nrf2 pathway. As expected, we found that ART promoted Nrf2 translocation to the nucleus and inhibited ferroptosis. Taken together, our findings, in conjunction with prior research, suggest that ART attenuates the development of NAFLD by inhibiting Nrf2-mediated ferroptosis.

Of course, although we found that ART could improve liver injury in NAFLD, there were still some deficiencies in this study. For example, some cell death markers were not detected, such as TUNEL staining in the liver. In addition, gender was not considered in the experiment. In the mechanistic research section, we explore ferroptosis as one of the major targets of ART for improving NAFLD. However, this part of the study has not been confirmed in vivo. These deficiencies will be addressed in future research.

Declarations

Author contribution statement

Qingyan Ye, Yun Jiang: Conceived and designed the experiments.

Di Wu, Jingwen Cai, Zhitian Jiang: Performed the experiments; Analyzed and interpreted the data.

Zhen Zhou, Liyan Liu, Qian Wang, Gang Zhao: Contributed reagents, materials, analysis tools or data.

Qihua Ling: Conceived and designed the experiments; Wrote the paper.

Funding statement

Dr. Qihua Ling was supported by National Natural Science Foundation of China {82004321}, Medical Innovation Research Special Project of Shanghai Science and Technology Commission {20Y21900300, 21Y11920500}, Budget project of Shanghai University of traditional Chinese Medicine {2022YJ-19}.

Data availability statement

Data will be made available on request.

Additional information

No additional information is available for this paper.

Ethics approval and consent to participate

Animal experimental procedures were approved by the Animal Ethics Committee of Shanghai Municipal Hospital of Traditional Chinese Medicine.

Declaration of competing interest

The authors declare that they have no known competing financial interests or personal relationships that could have appeared to influence the work reported in this paper.

Acknowledgements

Not Applicable.

References

- [1] E. Cobbina, F. Akhlaghi, Non-alcoholic fatty liver disease (NAFLD) - pathogenesis, classification, and effect on drug metabolizing enzymes and transporters, *Drug Metab. Rev.* 2 (49) (2017) 197–211, <https://doi.org/10.1080/03602532.2017.1293683>.
- [2] M. Eslam, L. Valenti, S. Romeo, Genetics and epigenetics of NAFLD and NASH: clinical impact, *J. Hepatol.* 2 (68) (2018) 268–279, <https://doi.org/10.1016/j.jhep.2017.09.003>.
- [3] J. Zhou, F. Zhou, W. Wang, X.J. Zhang, Y.X. Ji, P. Zhang, Z.G. She, L. Zhu, J. Cai, H. Li, Epidemiological features of NAFLD from 1999 to 2018 in China, *Hepatology* 5 (71) (2020) 1851–1864, <https://doi.org/10.1002/hep.31150>.
- [4] E. Roeb, A. Geier, Nonalcoholic steatohepatitis (NASH) - current treatment recommendations and future developments, *Z. Gastroenterol.* 4 (57) (2019) 508–517, <https://doi.org/10.1055/a-0784-8827>.
- [5] K. Gariani, F.R. Jornayvaz, Pathophysiology of NASH in endocrine diseases, *Endocr. Conn.* 2 (10) (2021) R52–R65, <https://doi.org/10.1530/EC-20-0490>.
- [6] Y.L. Fang, H. Chen, C.L. Wang, L. Liang, Pathogenesis of non-alcoholic fatty liver disease in children and adolescence: from "two hit theory" to "multiple hit model", *World J. Gastroenterol.* 27 (24) (2018) 2974–2983, <https://doi.org/10.3748/wjg.v24.i27.2974>.
- [7] S. Marchisello, A. Di Pino, R. Scicali, F. Urbano, S. Piro, F. Purrello, A.M. Rabuazzo, Pathophysiological, molecular and therapeutic issues of nonalcoholic fatty liver disease: an overview, *Int. J. Mol. Sci.* 8 (20) (2019), <https://doi.org/10.3390/ijms20081948>.
- [8] H. Hosseini, M. Teimouri, M. Shabani, M. Koushki, R. Babaei Khorzoughi, F. Namvarjah, P. Izadi, R. Meshkani, Resveratrol alleviates non-alcoholic fatty liver disease through epigenetic modification of the Nrf2 signaling pathway, *Int. J. Biochem. Cell Biol.* 119 (2020), 105667, <https://doi.org/10.1016/j.biocel.2019.105667>.
- [9] L.C. Meng, J.Y. Zheng, Y.H. Qiu, L. Zheng, J.Y. Zheng, Y.Q. Liu, X.L. Miao, X.Y. Lu, Salvianolic acid B ameliorates non-alcoholic fatty liver disease by inhibiting hepatic lipid accumulation and NLRP3 inflammasome in ob/ob mice, *Int. Immunopharm.* 111 (2022), 109099, <https://doi.org/10.1016/j.intimp.2022.109099>.
- [10] E.S. Lee, M.H. Kwon, H.M. Kim, H.B. Woo, C.M. Ahn, C.H. Chung, Curcumin analog CUR5-8 ameliorates nonalcoholic fatty liver disease in mice with high-fat diet-induced obesity, *Metabolism* 103 (2020), 154015, <https://doi.org/10.1016/j.metabol.2019.154015>.
- [11] Z. Lyu, X. Ji, G. Chen, B. An, Atractylodin ameliorates lipopolysaccharide and d-galactosamine-induced acute liver failure via the suppression of inflammation and oxidative stress, *Int. Immunopharm.* 72 (2019) 348–357, <https://doi.org/10.1016/j.intimp.2019.04.005>.
- [12] N. Muhamad, T. Plengsuriyakarn, C. Chittasupho, K. Na-Bangchang, The potential of atractylodin-loaded PLGA nanoparticles as chemotherapeutic for cholangiocarcinoma, *Asian Pac. J. Cancer Prev. APJCP* 4 (21) (2020) 935–941, <https://doi.org/10.31557/APJCP.2020.21.4.935>.
- [13] Y. Dong, X. Zhang, C. Yao, R. Xu, X. Tian, Atractylodin attenuates the expression of MUC5AC and extracellular matrix in lipopolysaccharide-induced airway inflammation by inhibiting the NF-kappaB pathway, *Environ. Toxicol.* (2021), <https://doi.org/10.1002/tox.23311>.
- [14] H.S. Chae, Y.M. Kim, Y.W. Chin, Atractylodin inhibits interleukin-6 by blocking NPM-ALK activation and MAPKs in HMC-1, *Molecules* 9 (21) (2016), <https://doi.org/10.3390/molecules21091169>.
- [15] T. Hirschhorn, B.R. Stockwell, The development of the concept of ferroptosis, *Free Radic. Biol. Med.* 133 (2019) 130–143, <https://doi.org/10.1016/j.freeradbiomed.2018.09.043>.
- [16] K. Hadian, B.R. Stockwell, SnapShot: ferroptosis, *Cell* 5 (181) (2020) 1188–1188 e1, <https://doi.org/10.1016/j.cell.2020.04.039>.
- [17] J. Qi, J.W. Kim, Z. Zhou, C.W. Lim, B. Kim, Ferroptosis affects the progression of nonalcoholic steatohepatitis via the modulation of lipid peroxidation-mediated cell death in mice, *Am. J. Pathol.* 1 (190) (2020) 68–81, <https://doi.org/10.1016/j.ajpath.2019.09.011>.
- [18] X. Li, T.X. Wang, X. Huang, Y. Li, T. Sun, S. Zang, K.L. Guan, Y. Xiong, J. Liu, H.X. Yuan, Targeting ferroptosis alleviates methionine-choline deficient (MCD)-diet induced NASH by suppressing liver lipotoxicity, *Liver Int.* 6 (40) (2020) 1378–1394, <https://doi.org/10.1111/liv.14428>.
- [19] P. Liu, D. Wu, J. Duan, H. Xiao, Y. Zhou, L. Zhao, Y. Feng, NRF2 regulates the sensitivity of human NSCLC cells to cystine deprivation-induced ferroptosis via FOCAD-FAK signaling pathway, *Redox Biol.* 37 (2020), 101702, <https://doi.org/10.1016/j.redox.2020.101702>.
- [20] A. Mohs, T. Otto, K.M. Schneider, M. Peltzer, M. Boekschoten, C.H. Holland, C.A. Hudert, L. Kalveram, S. Wiegand, J. Saez-Rodriguez, T. Longerich, J. G. Hengstler, C. Trautwein, Hepatocyte-specific NRF2 activation controls fibrogenesis and carcinogenesis in steatohepatitis, *J. Hepatol.* 3 (74) (2021) 638–648, <https://doi.org/10.1016/j.jhep.2020.09.037>.

- [21] P. Farzanegi, A. Dana, Z. Ebrahimpoor, M. Asadi, M.A. Azarbayjani, Mechanisms of beneficial effects of exercise training on non-alcoholic fatty liver disease (NAFLD): roles of oxidative stress and inflammation, *Eur. J. Sport Sci.* 7 (19) (2019) 994–1003, <https://doi.org/10.1080/17461391.2019.1571114>.
- [22] L. Shojaie, A. Iorga, L. Dara, Cell death in liver diseases: a review, *Int. J. Mol. Sci.* 24 (21) (2020), <https://doi.org/10.3390/ijms21249682>.
- [23] Z. Chen, R. Tian, Z. She, J. Cai, H. Li, Role of oxidative stress in the pathogenesis of nonalcoholic fatty liver disease, *Free Radic. Biol. Med.* 152 (2020) 116–141, <https://doi.org/10.1016/j.freeradbiomed.2020.02.025>.
- [24] D. Li, D. Zhao, J. Du, S. Dong, Z. Aldhamin, X. Yuan, W. Li, H. Du, W. Zhao, L. Cui, L. Liu, N. Fu, Y. Nan, Heme oxygenase-1 alleviated non-alcoholic fatty liver disease via suppressing ROS-dependent endoplasmic reticulum stress, *Life Sci.* 253 (2020), 117678, <https://doi.org/10.1016/j.lfs.2020.117678>.
- [25] H.J. Kim, Y. Lee, S. Fang, W. Kim, H.J. Kim, J.W. Kim, GPx7 ameliorates non-alcoholic steatohepatitis by regulating oxidative stress, *BMB Rep.* 6 (53) (2020) 317–322.
- [26] Y. Geng, A. Hernandez Villanueva, A. Oun, M. Buist-Homan, H. Blokzijl, K.N. Faber, A. Dolga, H. Moshage, Protective effect of metformin against palmitate-induced hepatic cell death, *Biochim. Biophys. Acta, Mol. Basis Dis.* 3 (1866) (2020), 165621, <https://doi.org/10.1016/j.bbadis.2019.165621>.
- [27] S. Tsurusaki, Y. Tsuchiya, T. Koumura, M. Nakasone, T. Sakamoto, M. Matsuoka, H. Imai, C. Yuet-Yin Kok, H. Okochi, H. Nakano, A. Miyajima, M. Tanaka, Hepatic ferroptosis plays an important role as the trigger for initiating inflammation in nonalcoholic steatohepatitis, *Cell Death Dis.* 6 (10) (2019) 449, <https://doi.org/10.1038/s41419-019-1678-y>.
- [28] L. Li, J. Fu, D. Liu, J. Sun, Y. Hou, C. Chen, J. Shao, L. Wang, X. Wang, R. Zhao, H. Wang, M.E. Andersen, Q. Zhang, Y. Xu, J. Pi, Hepatocyte-specific Nrf2 deficiency mitigates high-fat diet-induced hepatic steatosis: involvement of reduced PPARgamma expression, *Redox Biol.* 30 (2020), 101412, <https://doi.org/10.1016/j.redox.2019.101412>.